

Purification and biochemical characterization of simplified eukaryotic nitrate reductase expressed in *Pichia pastoris*[☆]

Guillaume G. Barbier,^{a,b} Rama C. Joshi,^a Ellen R. Campbell,^a
and Wilbur H. (Bill) Campbell^{a,b,*}

^a The Nitrate Elimination Company, Inc., Lake Linden, MI 49945, USA

^b Department of Biological Sciences, Michigan Tech University, Houghton, MI 49931, USA

Received 6 February 2004, and in revised form 7 May 2004

Available online 10 July 2004

Abstract

NAD(P)H:nitrate reductase (NaR, EC 1.7.1.1-3) is a useful enzyme in biotechnological applications, but it is very complex in structure and contains three cofactors—flavin adenine dinucleotide, heme-Fe, and molybdenum–molybdopterin (Mo–MPT). A simplified nitrate reductase (S-NaR1) consisting of Mo–MPT-binding site and nitrate-reducing active site was engineered from yeast *Pichia angusta* NaR cDNA (YNaR1). S-NaR1 was cytosolically expressed in high-density fermenter culture of methylotrophic yeast *Pichia pastoris*. Total amount of S-NaR1 protein produced was ~0.5 g per 10 L fermenter run, and methanol phase productivity was 5 µg protein/g wet cell weight/h. Gene copy number in genomic DNA of different clones showed direct correlation with the expression level. S-NaR1 was purified to homogeneity in one step by immobilized metal affinity chromatography (IMAC) and total amount of purified protein per run of fermentation was ~180 mg. Polypeptide size was ~55 kDa from electrophoretic analysis, and S-NaR1 was mainly homo-tetrameric in its active form, as shown by gel filtration. S-NaR1 accepted electrons efficiently from reduced bromphenol blue ($k_{\text{cat}} = 2081 \text{ s}^{-1}$) and less so from reduced methyl viologen ($k_{\text{cat}} = 159 \text{ s}^{-1}$). The nitrate K_M for S-NaR1 was $30 \pm 3 \mu\text{M}$, which is very similar to YNaR1. S-NaR1 is capable of specific nitrate reduction, and direct electric current, as shown by catalytic nitrate reduction using protein film cyclic voltammetry, can drive this reaction. Thus, S-NaR1 is an ideal form of this enzyme for commercial applications, such as an enzymatic nitrate biosensor formulated with S-NaR1 interfaced to an electrode system.

© 2004 Elsevier Inc. All rights reserved.

Keywords: Nitrate reductase; *Pichia pastoris*; *Pichia angusta*; Protein expression; Immobilized metal affinity chromatography; Gene copy number

NAD(P)H:nitrate reductase (NaR, EC 1.7.1.1-3) is the first enzyme in the nitrate assimilatory pathway of eukaryotic organisms, such as plants and fungi [1]. Eukaryotic assimilatory NaR can be reduced by NADH, NADPH, or both nucleotides, in the case of a bispecific enzyme, which catalyzes the reduction of NO_3^- to NO_2^- :



With a release of a large free energy, $\Delta G = -143 \text{ kJ/mol}$ and $\Delta E = 0.74 \text{ V}$, under standard conditions and pH 7, this redox reaction is essentially irreversible [1].

Holo NaR has a ~100 kDa polypeptide, which binds three different cofactors: molybdenum–molybdopterin (Mo–MPT), heme-Fe, and FAD in a ratio of 1:1:1 in three distinct and independently folding regions of the sequence (Fig. 1). NaR is found in homo-dimeric or homo-tetrameric catalytically active forms [2]. The Mo–MPT cofactor which is bound in the nitrate-reducing active site of NaR is found only in three families of enzymes: xanthine dehydrogenase family, sulfite oxidase (SOX) family, and the aldehyde dehydrogenase family [3,4]. A Cys residue bound to the molybdenum of the Mo–MPT cofactor characterizes the SOX family of enzymes (Fig. 2). Since NaR has high amino acid sequence homology with mammalian SOX [1,5], it is a member of the SOX

[☆] International patent pending, International application number PCT-US02-39341.

* Corresponding author. Fax: 1-906-487-3167.

E-mail address: bill@nitrate.com (W.H. (Bill) Campbell).

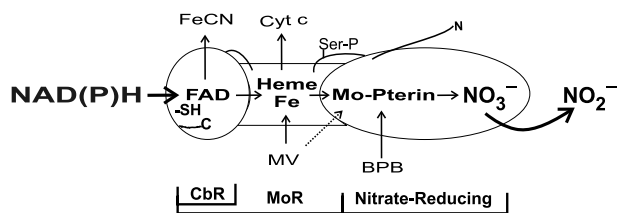


Fig. 1. Functional schematic for eukaryotic NaR monomeric subunit, as adapted from [1], showing the complete and partial reactions catalyzed by the enzyme. Abbreviations: CbR, cytochrome *b* reductase fragment; MoR, molybdenum reductase fragment; MV, reduced methyl viologen; BPB, reduced bromphenol blue; FeCN, ferricyanide; and Ser-(P), phosphorylation site.

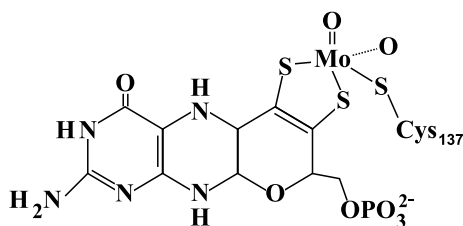


Fig. 2. Structure of Mo-MPT cofactor [1]. The Cys ligand to the Mo center is Cys137 in YNaR1 and S-NaR1.

family of Mo-MPT containing enzymes [1,3]. The biochemistry of assimilatory NaR has been studied in many respects, but no 3-D structure is available for the holo-NaR [1].

No commercial bacterial expression system was able to make an active eukaryotic holo NaR, because the prokaryotic Mo-MPT differs from the eukaryotic Mo-MPT: in prokaryotes, the Mo-MPT is conjugated to a nucleotide [3]. *Arabidopsis thaliana* NADH:nitrate reductase (AtNR2) was the first holo-NaR successfully expressed [6] in the methylotrophic yeast *Pichia pastoris*. Recently, a bispecific NAD(P)H assimilatory NaR was found in the yeast *Pichia angusta* (formerly *Hansenula polymorpha*) [7], called yeast nitrate reductase 1 (YNaR1), and successfully expressed in the *P. pastoris* expression system [8].

Sequence alignment of YNaR1 with the NaR model AtNR2 [1] showed that the two enzymes had the same

domain organization, which is defined in Table 1. The YNaR1 enzyme is composed of 859 amino acid residues and has five distinct domains. On the other hand, the 489 amino acid residue fragment of YNaR1 which constitutes simplified NaR or S-NaR1 contains only two of the five domains of holo-NaR (Table 1). The N_t region in YNaR1 is 30 residues long (positions 1–30). In AtNR2, it is thought to play a role in the stability and the regulation of the enzyme [1]. The YNaR1 Mo-MPT-binding domain is 240 residues long (positions 31–271). In the SOX refined structure, used as a model for the Mo-MPT-binding domain of NaR family [1,5], this domain is composed of 227 residues (positions 96–323) and contains nine α -helices and three β -sheets [5]. Cys 137 in YNaR1, which corresponds to Cys 191 in AtNR2, is predicted to be covalently bound to the molybdenum in the Mo-MPT cofactor (Fig. 2). The NO₃⁻ binding site may involve two positively charged amino acids, Arg 87 and Arg 142 in YNaR1, based on its alignment with SOX where the corresponding Arg residues were ligands to the substrate sulfite [5]. In YNaR1, the dimer interface domain (DI) is 165 residues long (positions 272–435) and was shown in AtNR2 to be essential for the formation of a stable and active dimer (unpublished data, W.H. Campbell). In SOX, the DI is 119 residues long (position 347–466) and contains two β -sheets [5]. In YNaR1, Hinge 1 is 65 residues long (positions 436–500). It links the DI domain to the cytochrome *b* domain (Cyt *b*). In AtNR2, Hinge 1 does not seem to have a defined secondary structure [1], but it contains a serine (Ser 534) involved in the regulation of the enzyme activity by the protein 14-3-3 [9]. No corresponding regulatory Ser is found in Hinge 1 of YNaR1. The sequence of S-NaR1 terminates in the middle of Hinge 1 and so it is made up of just the first two domains (Mo-MPT binding and DI domains) of the holo-enzyme, which are those essential for nitrate reducing activity and forming a structurally stable fragment [1].

The rate-limiting step in catalysis seems to involve the internal electron transfer from Cyt *b* to Mo-MPT, since the rates for these steps are about equal to the over k_{cat} of the whole enzyme [10,11]. It was observed

Table 1

Definition of the domains of YNaR1 and S-NaR1, based on the predicted domain structure of AtNR2 [1], showing amino acid sequence numbering and number of residues per defined region of the sequences

Enzyme	Sequence regions							
	Nt ^a	Mo-MPT	DI	Hinge 1	Cyt <i>b</i>	Hinge 2	FAD	NAD(P)H
AtNR2	1–90 (90)	91–334 (244)	335–490 (156)	491–540 (50)	541–620 (80)	621–660 (40)	661–780 (120)	781–917 (137)
YNaR1	1–30 (30)	31–271 (240)	272–435 (165)	436–500 (65)	501–577 (77)	578–594 (17)	595–720 (126)	721–859 (139)
S-NaR1	1–30 (30)	31–271 (240)	272–435 (165)	436–468 (32)	NP	NP	NP	NP

Note. S-NaR1 polypeptide is 489 residues long, but only 468 of these come from YNaR1 with the remainder from the expression vector.

^a Abbreviations: Nt, N-terminal sequence of NaR; Mo-MPT, molybdenum-molybdopterin cofactor binding domain; DI, dimer interface domain; Cyt *b*, cytochrome *b* domain; FAD, flavin adenine dinucleotide binding domain; NAD(P)H, nicotinamide adenine dinucleotide binding domain; and NP, not present.

by X-ray absorption spectroscopy of AtNR2 that interactions between Mo and one of its three Mo–S ligands (Fig. 2) in the resting enzyme are different than in the active enzyme [12]. Structural changes of the Mo–S ligand seem to be induced by the catalytic turnover of the NaR [1,10,12]. The size and the complexity of the NaR enzyme makes the in-depth study of its catalytic mechanism difficult to do and interpret. Clearly, if the nitrate-reducing active site of NaR could be studied independent of internal electron transfer and the structural components required for this functionality, namely the Cyt *b*, FAD, and NAD(P)H domains as well as Hinge 1 and 2, it might be possible to gain unique insight into the key characteristics of NaR catalysis.

Mild proteolytic degradation showed that the NaR is composed of independently functional domains and since these domains are linearly arrayed in the NaR gene, it appeared that recombinant expression of enzyme fragments might be possible [1]. The first active NaR fragment successfully expressed in *Escherichia coli* and crystallized was the cytochrome *b* reductase (CbR) fragment [13,14], which contains the NADH-binding domain and the FAD-binding domain and catalyzes ferricyanide reductase activity (Fig. 1). A NaR fragment showing a cytochrome *c* reductase activity, the molybdopterin reductase fragment (MoR) (Fig. 1), was successfully cloned and expressed in *E. coli* [15]. The MoR and MoR+ fragment (MoR+ = MoR plus dimer interface domain, Fig. 1) from corn and spinach were successfully expressed at high level by fermentation in the methylotrophic yeast *P. pastoris* [16], which does not assimilate nitrate and does not possess an NaR activity [5,8]. Furthermore, a chimera MoR fragment was made by fusion of a rat Cyt *b*₅ with spinach NaR's CbR [17], confirming the modularity of the enzyme. Having access to purified NaR fragments has advanced the understanding of mechanistic aspects of the catalytic process and structure of NaR [13–16]. However, the structure of the nitrate-reducing fragment of NaR and its active site remains unknown.

Here, to make the nitrate-reducing functionality of NaR more accessible, we engineered an eukaryotic yeast nitrate reductase in order to obtain a simplified NaR fragment, which is called S-NaR1, capable of specific nitrate reduction when in contact with an electron donor, and expressed it in large quantity by fermentation in the methylotrophic yeast *P. pastoris*. This simplified fragment is easier to produce and purify, and more stable than the holo-NaR due to its smaller size and to its lower degree of complexity with Mo–MPT as its only cofactor. S-NaR1 could be used in commercial applications of NaR like a nitrate biosensor [18] in which catalytic efficiency with specificity and stability are important parameters.

Materials and methods

Construction of the YNaR1-pPICZb

All the restriction enzymes used were provided by New England Biolabs (NEB, Beverly, MA). The cDNA fragment encoding the NAD(P)H:NaR of *P. angusta* (YNaR1) in the pBSII-SK vector (Stratagene, La Jolla, CA) was a kind gift from Siverio and co-workers [7]. A 2735-bp *EcoRI*–*KpnI* fragment containing the YNaR1 ORF was subcloned under the control of the alcohol oxidase 1 (AOX1) methanol inducible promoter in the *P. pastoris* Zeocin resistant expression vector pPICZ-b (Invitrogen, Carlsbad, CA) [8]. The plasmid obtained was called YNaR1-pPICZb and its size was 6029 bp [8]. Sequence encoding YNaR1 polypeptide has GenBank Accession No. Z49110.

Construction of the S-NaR1-pPICZb

The YNaR1-pPICZb plasmid was digested for 16 h at 37 °C with the restriction enzyme *XbaI*. The digestion products were separated on a 0.7% low melting point agarose gel, and five fragments were obtained: one composed of 4683 bp containing the pPICZ-b DNA sequence and the YNaR1 DNA sequence coding for *N_t* region, the nitrate reducing fragment (Mo–MPT binding and DI domains), and part of Hinge 1 and four other fragments (454, 149, 441, and 299 bp). The 4683 bp DNA fragment was extracted from the agarose gel using a GELase (Epicentre Technologies, Madison, WI), purified with Promega PCR prep wizard kit (Promega, Madison, WI), and ligated overnight at room temperature with a T4 DNA ligase (NEB, Beverly, MA). The resulting plasmid contained a 1417 bp DNA sequence from the YNaR1 cDNA coding for the nitrate reducing fragment, in-frame with hexa-His-tag and the stop codon built into the pPICZ-b vector, yielding to a 1486 bp expression cassette. Both plasmids (YNaR1-pPICZb and SNaR1-pPICZb) obtained were transformed in Epicurian Coli XL1-blue cells (Stratagene, La Jolla, CA) and after amplification, the plasmid was purified with Wizard Plus minipreps (Promega, Madison, WI). The sequence encoding S-NaR1 has GenBank Accession No. AY541702.

Pichia pastoris electrotransformation and screening

Preparation of wild-type *P. pastoris* competent cells and electrotransformations were done according to the protocol described previously [6,16]: 5 µg of purified plasmids was linearized with the *SacI* restriction enzyme and 1 µg of this DNA was used to transform by electroporation the *P. Pastoris* competent cells. The electrotransformation solution was spread on YPDS plates

with 1000 μg Zeocin/mL. From these plates, 10–50 clones were picked up and used to inoculate a 3 mL minimum glycerol media (MGY) culture tube with 1000 μg Zeocin/mL. After 16 h at 30 °C and 300 RPM, the 3 mL culture was used to inoculate 100 mL MGY flask culture. After 24 h of growth at 30 °C and 300 RPM, the cells were harvested by centrifugation (3000g, 5 min, 4 °C) and resuspended in expression media supplemented with 2 mL of 100 mM disodium molybdate according to the method previously described [16,19]. Methanol was added, and after 24 h of induction time at 30 °C and 300 RPM, yeast cells were harvested (10,000g, 10 min, 4 °C) and resuspended in extraction buffer [16]. Yeast cells resuspended were then mixed with 0.5 mm zirconium beads and lysed with a Mini Bead-Beater (Biospec products, Bartlesville, OK), since the protein was expressed internally. Crude extracts were centrifuged (10,000g, 10 min, 4 °C), and the NaR activity was assayed with dithionite-reduced methyl viologen (MV) as electron donor [1,2]. The S-NaR1 *P. pastoris* cell line with the best product activity per g of wet cell weight (wcw) yield ($Y_{P/X}$) was selected for fermentation studies. A *P. pastoris* YNaR1-expressing cell line was processed as described above for a comparative control and its NaR activity was assayed with NADH as electron donor.

Reduced dye NaR assay

A volume of enzyme (1–20 μL) was pipetted into a tube that contained 2 mL of assay buffer. The final concentration in the reaction tube was: 25 mM potassium phosphate, pH 7.5, 10 mM potassium nitrate, 0.5 mM methyl viologen (MV) or 0.2 mM bromphenol blue (BPB), and 5 mM sodium dithionite. The reaction was carried out at 30 °C and was stopped after 1 min by air oxidation via mixing on a Vortex followed by addition of 1 mL of color reagent 1 (10 g sulfanilamide/L of 3 N HCl). After mixing, 1 mL of color reagent 2 (0.2 g/L of *N*-naphthylethylenediamide) was added and mixed. After 5 min of development, the absorbance at 540 nm was read in a spectrophotometer calibrated with nitrite standards. This standard curve was used to convert A_{540} values to nmol nitrite formed. In time course assays, the unit of NaR was 1 μmol nitrite formed per min per amount of enzyme.

Methanol utilization phenotype determination

The methanol utilization (Mut) phenotype was determined by streaking the expressing cell lines on minimum media with methanol according to the protocol previously described [20]. The growth was evaluated after three days at 30 °C. *P. pastoris* cell lines of known phenotype were used as standards (Mut⁺, wild-type *P. pastoris*; Mut^S, KM71H *P. pastoris* strain).

Determination of gene copy number by slot blot

The yeast genomic DNA was prepared using the MasterPure Yeast DNA kit (Epicentre, Madison, WI). One microgram of purified genomic yeast DNA and 0.2 ng of each of the following plasmids, S-NaR1-pPICZb and pPIC9 (Invitrogen, Carlsbad, CA), which contained, respectively, 1 copy of the S-NaR1 gene and 1 copy of the HIS4 gene, were immobilized on positively charged nylon membrane (Roche, Basel, Switzerland) according to the manufacturer's recommendations of the slot blot apparatus (Bethesda Research Laboratory, Gaithersburg, MD). The DNA was cross-linked to the membrane by 10 min of UV exposure. Two sets of hybridizations for each probe (copy number probe and control probe) were done by using the Easy Hyb kit from Roche and an Isotemp incubator (Fisher Scientific, Pittsburg, PA). The DIG wash and Block buffer kits from Roche were used (Roche DIG easy hyb kit, Roche, Basel, Switzerland). The color development was done using the DIG DNA Detection kit from Roche. The slot blots were then scanned and the density of the slot blot was analyzed by using Photoshop software (Adobe Systems, San Jose, CA). The intensity data of the slot blot probed by the copy number probe were then matched against the intensity data obtained with the slot blot probed with the one copy control, which was the HIS4 based probe [20,21].

Slot blot gene probe design

The S-NaR1 probe was used to analyze the number of copies integrated to the *P. pastoris* genome by homologous recombination events [20,21]. It was constructed by using the PCR DIG labeling mix^{plus} kit purchased from Roche (Roche, Basel, Switzerland). The 5' primer was the 21 bp oligonucleotide, 5' CCGAGGT GCTTCCAACAGATC 3', matching the region 1061–1081 of the SNaR1-pPICZb plasmid. The 3' oligonucleotide primer was composed of 43 bp and had the following sequence:

5' CTTGACCCTATCCATCCAACCGCCAGGCT TGTTGGCCACCACG 3'. It matched the region 2301–2343 of the pPICZb-SNaR1 plasmid. The template used was the pPICZb-SNaR1 plasmid and the final product had a length of 1283 bp (positions 1061–2343 on SNaR1-pPICZb). The one copy only control was based on the HIS4 gene from *P. pastoris* and labeled as previously described with the DIG non-radioactive marker. The 41 bp 5' primer had the following composition: 5' GCGGTGAGCATCTAGACCTTCCAGCAGCCA GATCCATCAC 3'. The 36 bp 3' primer had the following sequence: 5'GCTGACCAGCTTGACCCTG ATCGTTCACCTCTCGAC3'. The DNA template used was the pPIC9 plasmid (Invitrogen, Carlsbad, CA). The

PCRs were run according to the kit manufacturer's recommendations.

S-NaR1 *P. pastoris* cell line fermentation

Three fermentations of the selected S-NaR1 *P. pastoris* cell lines were run. Starter cultures of the S-NaR1 *P. pastoris* cell lines were grown in 3 mL MGY plus 1000 µg/mL Zeocin for 16 h, 300 RPM, 30 °C. After 16 h, the two 3 mL cultures were aseptically transferred to two 100 mL MGY plus 100 µg/mL Zeocin culture for 16 h, 300 RPM, 30 °C. Then, the two 100 mL MGY culture were aseptically transferred to two 500 mL MGY in 2.8 L Fernbach flasks. The two 500 mL cultures were aseptically transferred to the fermenter when a biomass of ~ 80 g/L of wcv was achieved (16 h at 300 RPM, 30 °C). The fermenter was filled with 5.5 L glycerol minimal media [16,22]. The fermentation was conducted in a BioFlo3000 fermenter (New Brunswick Scientific, Edison, NJ) with a working volume vessel of 10 L, as previously described [16]. The fermenter was interfaced to a computer using the NBS-BioCommand software package (New Brunswick Scientific, Edison, NJ). The fermenter was operated at 30 °C, the pH was maintained at 4.9 by addition of 28% NH₄OH, and the dissolved oxygen level was kept above 35% by using the DO cascade loop of the fermenter. If necessary, pure oxygen was used to maintain the oxygen set point. The glycerol and the methanol inputs were monitored by using a balance (Denver Instrument, Arvada, CO) interfaced to a computer via the Winwedge Pro software (Tal Technologies, Philadelphia, PA).

The standard fermentation procedure followed was in three steps [16,22]. First, the batch mode in which, based on previous fermentations, the yeast consumed all of the glycerol initially present in 15 h (from t_0 to t_{15}), and grew according to the general Eq. (1) under substrate limiting conditions

$$X_t = X_0 \times e^{\mu t}, \quad (1)$$

where X_t is biomass at time t (g), X_0 is initial biomass (g), μ is growth rate (h^{-1}), and time = $0 < t \leq 15$ h.

A waiting period of time of about 1 h between t_{15} and t_{16} was allowed before starting the glycerol feed batch. The fermenter culture was grown for 8 h (from t_{16} to t_{24}), with a 50%, w/v glycerol solution supplemented with a 12 mL/L PTM4 trace salt solution [16]. The glycerol feed was started at t_{16} and the flow rate was proportionally increased to follow the yeast culture glycerol maximal growth rate (Eq. (2))

$$F_t = X_t \times C_G, \quad (2)$$

where F_t is flow rate (g/h) at time t with $16 < t \leq 24$, X_t is biomass at time t (g), and C_G is yeast glycerol consumption rate (g glycerol/g wcv/h).

Therefore, applying the general growth equation, F_t was increased hourly according to Eq. (3)

$$F_t = X_{t_{15}} \times e^{\mu t} \times C_G, \quad (3)$$

where time = $16 < t \leq 24$ and $X_{t_{15}}$ is the biomass at t_{15} . The growth factor μ was fixed between t_{16} and t_{24} at 0.10 h^{-1} in order to reach, in 8 h, a target biomass $X_{t_{24}}$ of 1600 g wcv.

At t_{24} the feed batch was stopped and the culture was starved for 1 h in order to use all the glycerol (sole carbon source). Finally at t_{25} , the fermenter culture was fed with 100% methanol HPLC grade (Becton and Dickinson, Franklin Lakes, NJ, USA) supplemented with 12 mL/L PTM₄ trace salt solution as the sole carbon source in order to induce protein expression. The methanol feed rate was adjusted (from t_{25} to t_{45}) according to Eq. (3) with the corresponding methanol parameters and checked by the "oxygen spike" method using the dissolved oxygen probe in the fermenter [16,22].

Cell growth was monitored at 600 nm and by recording the wcv. One milliliter of fermentation solution sample was centrifuged for 2 min in a pre-weighted microcentrifuge tube at 12,000 RPM, 4 °C. The supernatant was discarded and the wcv was recorded. The microcentrifuge tube was then filled to 1 mL with cold extraction buffer and 0.5 mm zirconium beads and processed with the Mini Bead-Beater as described above. The MV-NaR activity was assayed and recorded. When the production of S-NaR1 began to level off, the culture was harvested and the cells were centrifuged for 10 min at 10,000 RPM, 4 °C, resuspended in extraction buffer (50 mM sodium phosphate, 0.3 M NaCl, 1.5% w/v polyethylene glycol, 10% glycerol, and 10 mM imidazole, pH 7.3), and stored at -80 °C.

Large scale crude extract preparation and purification

The resuspended cells were thawed overnight at 4 °C, centrifuged, and resuspended in a minimum volume of the extraction buffer described above (~2 L of buffer/kg wcv). *P. pastoris* cells were broken by passing the suspension twice through the 0.6 L chamber of a Dyno-Mill type KDL A (Glen Mills, Clifton, NJ) filled with half a liter of 0.5 mm glass beads at a flow rate of 10 L/h [10,16]. The Dyno-Mill was cooled by a CFT-300 chiller (Neslab, Portsmouth, NH) set at -5 °C, in order not to exceed an outlet temperature of 5 °C. After the second pass, the crude extract was centrifuged for 15 min at 15,000 RPM, 4 °C [16].

The centrifuged crude extract (CCE) was purified with 400 mL immobilized metal affinity chromatography (IMAC), a Talon Superflow resin (Clontech laboratories, Palo Alto, CA) loaded with Co²⁺. The protocol followed was similar to that of the batch-binding process described by the manufacturer in the Talon resin manual: after mixing the gel and the CCE for 1 h, the gel

was recovered on a filter funnel. The gel was then washed in 10 bed volumes of purification buffer (same composition as extraction buffer) and recovered on a filter funnel. This stage was repeated six times. The gel was poured into a 1 L glass column and processed with the elution buffer (50 mM sodium phosphate, 0.3 M NaCl, 10% glycerol, and 150 mM imidazole, pH 7.3). The fractions containing the highest MV-NaR activity were pooled and buffer exchanged into a Mops buffer (25 mM Mops, pH 7.0) on an Amicon unit (Amicon, Danvers, MA) with a 30,000 kDa cut-off membrane. Concentration of protein was determined at 280 nm on UV, Vis spectrophotometer HP 8452A diode array spectrophotometer using a coefficient factor ($\epsilon_{\text{S-NaR1}} = 120,000 \text{ M}^{-1} \text{ cm}^{-1}$) determined from the predicted amino acid sequence with the Protparam program available on the Expassy website (<http://us.expassy.org/tools/protparam.html>).

Molecular weight determination

A 4–20% gradient Nu-PAGE (Invitrogen, Carlsbad, CA) under denaturing and reducing conditions was performed to determine the molecular weight of the monomer, as previously described [2,16]. Gel-exclusion chromatography was performed on Sepharose 4B (Amersham Biosciences AB, Uppsala, Sweden) to determine the degree of polymerization of the active form. The buffer used was a 50 mM sodium phosphate, 100 mM NaCl, pH 7.5, and fractions of 8 mL were collected. MV-NaR assays were performed and the A_{280} was measured.

K_M and k_{cat} determination with different electron donors

The NaR activity of S-NaR1 was measured using methyl viologen and bromphenol blue as an electron donor as described above, but the final concentration in the reaction tube was varied from 10 to 500 μM nitrate. The concentration of protein was determined at 280 nm, as described above.

Cyclic voltammetry

Purified S-NaR1 and commercial natural corn leaf (*Zea mays*) NADH:NaR (The Nitrate Elimination, Lake Linden, MI) were formulated as protein films on commercial pyrolytic graphite edge-plane electrodes (Pine Instrument, Grove City, PA) using polymyxin B sulfate (Sigma Chemical, St. Louis, MO) as a promoter for film formation and 25 mM Mops buffer at pH 7.0 and 22 °C, under purified high-purity argon gas. The protein film on the electrode was formed in a manner similar to that used previously [23]. Cyclic voltammograms were run in the presence and absence of nitrate ions in an anaerobic buffered system at various poten-

tials which were compared to the Standard Hydrogen Electrode [23]. The electrode system was linked to a computer using the BAS CV 50 W interface and software (Bioanalytical systems, West Lafayette, IN). The voltammograms were normalized to the same control response curve to compensate for differences in experimental conditions.

Results and discussion

Generation of S-NaR1-expressing *P. pastoris* cell lines

Purified YNaR1-pPICZb plasmid was digested with *Xba*I and the digestion products were separated on a 0.7% agarose gel. The size of the largest fragment observed (~4.7 kb) after *Xba*I digestion matched the in silico predicted size (4683 bp) for the core plasmid plus the code for S-NaR1. The 4.7 kb fragment was purified from the agarose gel, ligated with a T4 DNA ligase, and amplified in *E. coli*. It was designated the SNaR1-pPICZb plasmid. Restriction mapping of the purified amplified S-NaR1 plasmid and agarose gel electrophoresis of the restriction digestions were done. The results observed matched the in silico predictions (Fig. 3). The SNaR1-pPICZb plasmid was transformed by electroporation into wild-type *P. pastoris* competent cells to generate putative S-NaR1-expressing *P. pastoris* cell lines.

S-NaR1 expressing *P. pastoris* cell line selection

From the YPDS plates plus Zeocin, 20 *P. pastoris* colonies were picked up and grown in MGY media plus Zeocin in 3 mL culture tubes. The MGY media are a *P. pastoris* selective minimum media with glycerol as

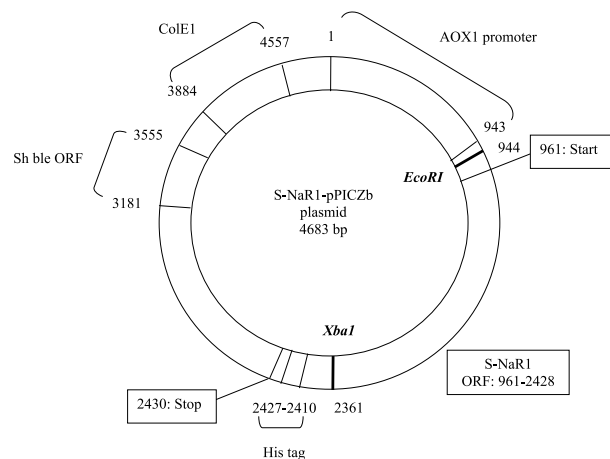


Fig. 3. The SNaR1-pPICZb expression vector construct. Abbreviations: AOX1, methanol inducible promoter; Sh Bleo ORF, Zeocin resistance gene; and ColE1, origin of replication in *E. coli*.

sole carbon source. These media supplemented with Zeocin were used instead of the regular glucose based media to grow *P. pastoris* strains prior to induction. Protein expression was induced by methanol in 100 mL flask expression media culture flasks and crude extracts were prepared from the cells obtained in these cultures, after the yield of wcv was determined. The 20 S-NaR1 *P. pastoris* cell lines screened had MV-NaR activity per g wcv yield ($Y_{P/X}$) ranging from 0.05 to 0.5 U/g. The cell line with the highest $Y_{P/X}$ was selected for fermentation. Since NaR activity was observed in the extracts of the *P. pastoris* cell lines, the cells must have incorporated the Mo–MPT cofactor (Fig. 2) into the S-NaR1 polypeptide which resulted in a stable, catalytic combination.

Genomic slot blot analyses were done on the 20 *P. pastoris* S-NaR1 cell lines (Fig. 4) to determine if the expression level of protein was limited by one of the following events: transcription level, Mo–MPT cofactor biosynthesis, or by insertion of the Mo–MPT into the S-NaR1 apoprotein, since *P. pastoris* is not known to produce a Mo–MPT containing enzyme naturally. The S-NaR1 copy number probe used was the 1283 bp coding sequence (positions 1061–2343 in SNaR1-pPICZb plasmid) of the YNaR1 cDNA coding for the Mo–MPT domain (Fig. 4A). The HIS4 gene of *P. pastoris* was used as a one copy control in the slot blot analysis (Fig. 4B), since it has been shown that this gene was present in only one copy in the yeast genome [20,21]. The results of the two sets of slot blots were matched and normalized by dividing the value of the band intensity of a given clone by the S-NaR1 based probe (Fig. 4A) over the value of the band intensity of the same clone probed by the HIS4 based probe (Fig. 4B). Then, for each S-NaR1 *P. pastoris* cell line, its $Y_{P/X}$ was plotted against the number of copies of the S-NaR1 found in the genomic DNA by slot blot analysis (data not shown). We found a direct correlation between the copy number of the S-NaR1 gene integrated in the

yeast genome and the level of protein expression in 100 mL shake flask culture (data not shown). The two screening methods led to the same results: the S-NaR1 cell line with the highest MV NaR activity (0.5 U/g wcv) had the greatest number of gene copies integrated in the genome (~3). It has been shown that the number of gene copies integrated in the yeast genome generally correlates with the gene expression level [21,24]. Copy number of gene integrated in the yeast genomic DNA can go up to 15 copies for small genes [21,24], but a lower limit may exist with larger genes like NaR. The observed results indicated that the limiting event for expression of NaR activity in *P. pastoris* seemed to be the accessibility of the gene, that is to say, the number of copies integrated into the yeast genome, rather than some aspect of the availability of the Mo–MPT cofactor or its insertion into the S-NaR1 polypeptide.

The S-NaR1 expressing methanol utilization phenotype was determined according to the general protocol previously described [16,20]. The growth on minimum media plus methanol showed that the selected YNaR1 and the S-NaR1 *P. pastoris* cell lines were growing as fast as the wild type strain. Therefore, these clones were methanol utilization positive (Mut^+), which was expected based on the use of wild-type *P. pastoris* as the host cell line and the integration mechanism for the pPICZ vectors [19].

Fermentation of S-NaR1-expressing *P. pastoris* cell line

The fermentations were conducted according to the standard protocol described in the Materials and methods section and used previously for fermentation of NaR-expressing *P. pastoris* cell lines [8,10,16]. The fermenter employed was a 10 L working volume Bioflo 3000. Two 500 mL MGY starter cultures of S-NaR1 *P. pastoris* cell line #1 were used to inoculate the fermenter with an initial biomass (X_0) of 90 g wcv, and the total initial volume of the fermenter was 6.7 L. The data for one fermentation run of the S-NaR1 *P. pastoris* cell line #1 are presented in Fig. 5, which is representative of several fermentation runs done with this cell line and other S-NaR1-expressing cell lines. During the glycerol batch mode (t_0 – t_{15}), the growth rate μ was 0.12 h^{-1} , the yield of g wcv per gram of glycerol ($Y_{X/G}$) was 2.3 g/g, and the glycerol consumption rate was 0.32 g glycerol/g wcv/h. The total mass of wet cells at the end of the glycerol batch was ~650 g. After 1 h of starvation between the glycerol batch and fed batch, the glycerol feed was started at t_{16} . The growth rate μ was fixed at 0.10 h^{-1} in order to reach the target biomass of 1600 g wcv in 8 h. The estimated glycerol flow rate (F_g) starting point was calculated according to Eq. (3) and was equal to 64 g of glycerol solution/L/h, and increased.

After 8 h of glycerol feed batch from t_{16} to t_{24} , the yeast cells were starved for 1 h in order to use the last

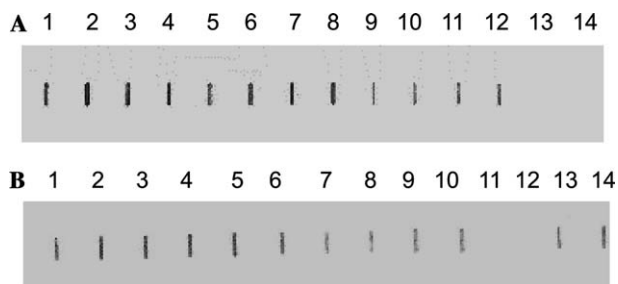


Fig. 4. Genomic DNA slot blots for S-NaR1 gene copy number determination of different clones. For each slot, 1 μ g of purified genomic DNA and 0.2 ng of purified plasmid for the controls were used. Lanes 1 and 2: S-NaR1 clone a; lanes 3 and 4: S-NaR1 clone b; lanes 5 and 6: S-NaR1 clone c; lanes 7 and 8: S-NaR1 clone d; lanes 9 and 10: S-NaR1 clone e; lanes 11 and 12: SNaR1-pPICZb plasmid control; and lanes 13 and 14: pPIC9 plasmid. (A) Slot blot probed with S-NaR1. (B) Slot blot probed with His 4.

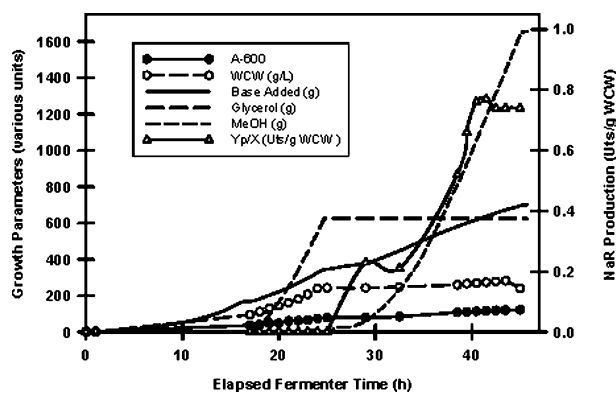


Fig. 5. Fermentation of S-NaR1 *P. pastoris* cell line 1. The filled circle indicates the absorbance at 600 nm (A_{600}). The open circle represents the wet cell weight or WCW (g/L). The open triangle is for the NaR productivity: yield of product over biomass or $Y_{p/X}$ (MV NaR uts/g wcw). The long dashed line is for the glycerol added (g). The short dashed line shows the methanol added (g). The total base added to neutralize the culture to the pH set point is shown as a solid line. The last three parameters were taken from the Bio-Command software and represent readings taken directly from the fermenter at intervals of 1 min and therefore are shown as continuous lines.

trace of glycerol and methanol was fed to the culture. The methanol flow rate was adjusted every hour according to Eq. (3) with the specific parameters for methanol feed shown below, and checked with the DO spike method [16,22]. The maximum methanol consumption rate observed for this clone was 0.12 g methanol/g wcw/h, and the maximum μ obtained for cell line # 1 was known from previous fermentations to be 0.07 h^{-1} and the biomass used in Eq. (3) was X_{t25} . The μ was maintained at 0.02 h^{-1} in this fermentation, due to the heat transfer limitation of the fermenter. At t_{45} , the cells were harvested and the total biomass was 2150 g wcw, as expected. In the representative S-NaR1 cell line fermentation (Fig. 5), 1685 g of methanol was consumed during the induction phase and ~ 1445 MV-NaR units of S-NaR1 (~ 0.5 g of S-NaR1 protein based on the specific activity of purified enzyme) was produced. The $Y_{X/M}$ was 0.2 g wcw/g methanol, and the $Y_{P/X}$ was 0.74 MV-NaR units per gram of wcw (0.25 mg of protein/g wcw). The overall productivity (q_p) of the methanol induction phase of this fermentation was 0.019 MV-NaR U/g wcw/h (or $5 \mu\text{g}$ protein/g wcw/h).

Purification of S-NaR1

The centrifuged crude extract obtained from the two passes of the Dyno-Mill contained 1445 MV-NaR units and was mixed with Talon Superflow cobalt gel for 1.5 h at 4°C , and rinsed six times in a batch mode with 10 gel volumes of purification buffer. Around 99% of the active protein was bound to the gel, and 500 MV-NaR units of NaR activity was recovered after elution, representing

$\sim 33\%$ of recovery. The fractions containing the enzyme were pooled and buffer exchanged into Mops buffer and the amount of purified protein was estimated at 181 mg by the absorbance at 280 nm and derived extinction coefficient. The purification yield was about 30% and the buffer exchanged recovery was 99%.

Biochemical characterization

Molecular size analysis by denaturing polyacrylamide gel electrophoresis revealed a protein band at $\sim 55,000$ Da (Fig. 6) which is near the predicted size for the monomeric S-NaR1 (56,528 Da). When gel-exclusion chromatography (Fig. 7) was performed, 80% of the MV-NaR activity was recovered. The results showed one main peak at around 220 kDa and one smaller peak at ~ 110 kDa. The 220 kDa represented the homo tetrameric active form of the S-NaR1 protein, which seemed to be the most common form of the enzyme since the amount of protein based on the A_{280} was the highest. The 110 kDa peak represented a less common active homo dimeric form of the S-NaR1 catalytic enzyme. Natural holo-NaR is known to form a mixture of homo-dimers and tetramers [1,2]. The multimeric form of S-NaR1 was expected since the DNA sequence cloned contained the coding for the dimer interface domain of holo-NaR and it has been shown that NaR needs to be in an even homo multimeric form (dimeric or tetrameric) to be active [1,2,16].

The spectra of the purified S-NaR1 showed an absence of the 413 nm peak and of the 460 nm shoulder found in the spectra of the NaR holo-enzyme (Fig. 8). The 413 peak is known to be the α absorbance peak of heme-Fe in Cyt *b* and the 460 nm shoulder corresponds to the FAD cofactor [1,10,13,15]. Therefore, it can be concluded that S-NaR1 does not contain the C-terminal portion of holo-NaR containing the heme-Fe, flavin adenine dinucleotide, and pyridine nucleotide binding sites, which is consistent with its design. The S-NaR1 spectra revealed a shoulder at 290 nm (Fig. 8), which could be hypothesized to be attributed to the Mo-MPT cofactor but since its spectral characteristics in holo-NaR are not known, this needs to be verified.

Further investigations were done by using different electron donors. NADH, NADPH, reduced MV, and reduced BPB were used to characterize the catalytic activity of S-NaR1. As expected, no NaR activity was observed when S-NaR1 was in the presence of NO_3^- with NADH or NADPH as electron donor. Reduced dyes such as MV and BPB can drive the nitrate reduction of the holo-enzyme [1]. The electron acceptor sites for MV and BPB are thought to be the Mo-MPT. These catalytic activities, in the holo-NaR, are independent of functionality of the other domains. When S-NaR1 was assayed with BPB, the k_{cat} observed was 13 times higher than the MV k_{cat} (Table 2). No increase of the activity

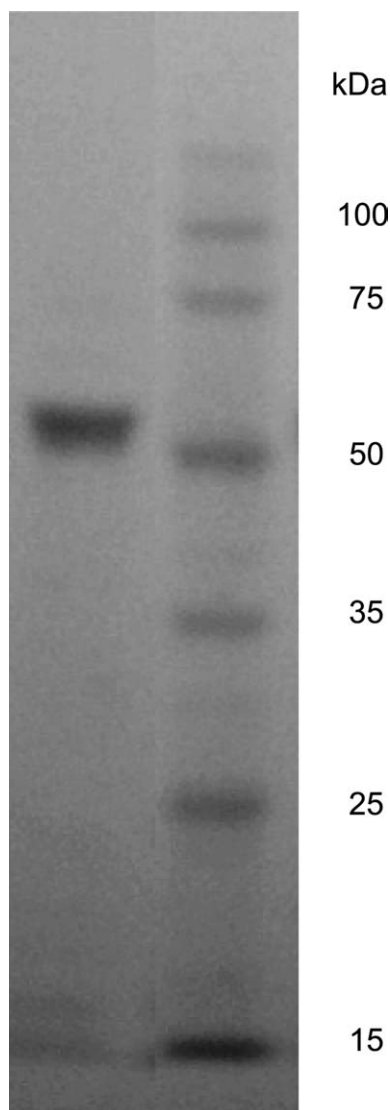


Fig. 6. Denaturing polyacrylamide gel for determination of the relative molecular size of the S-NaR1 polypeptide. A 4–20% gradient Nu-PAGE gel was used and the protein was purified by Talon gel IMAC, buffered exchanged, and concentrated. Approximately 1 µg was loaded on the gel and run for 2 h at 100 V. Lane 1, 1 µg S-NaR1 at ~55 kDa; and lane 2, protein standards of the relative molecular masses shown to the right of the gel (Sigma M-0671).

was observed when the MV concentration was increased (data not shown). Therefore, it can be concluded that the BPB electron acceptor site is more accessible in S-NaR1 than the MV electron acceptor site. The hypothesis is that in the NaR holo-enzyme, reduced BPB might donate its electrons preferentially to the Mo–MPT rather than via the heme–Fe in the Cyt *b* domain, and that MV might reduce preferentially the Cyt *b* domain (Fig. 1). However, it is clear from the results here that reduced MV can donate electrons directly to the Mo–MPT since S-NaR1 does not contain the Cyt *b* domain. However, the low rate of nitrate reducing ac-

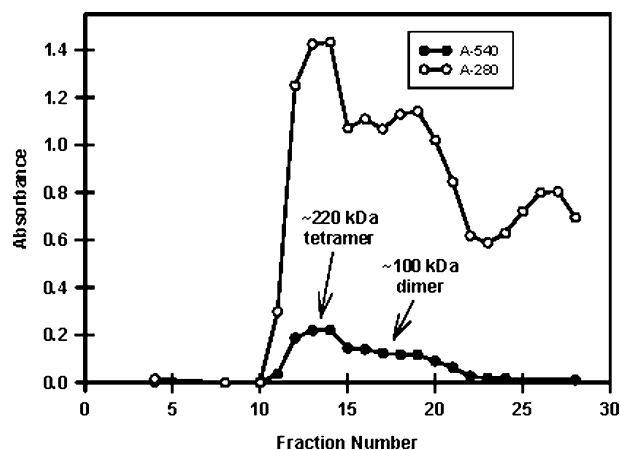


Fig. 7. Gel filtration of S-NaR1 on Sepharose 4B at 4 °C. Open circles represent the total protein absorbance at A_{280} nm. The filled circle represents the NaR activity determined at A_{540} nm in the MV-NaR activity assay. Fractions of 8 ml were collected and total recovery was 80% of applied NaR activity.

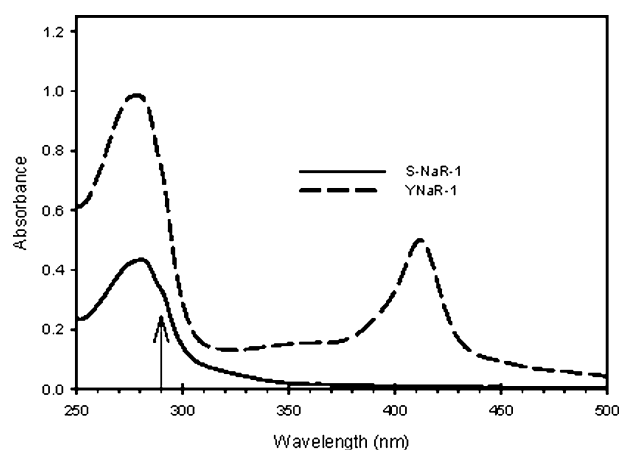


Fig. 8. UV/Visible spectra comparing S-NaR1 and YNaR1. The arrow at 290 nm indicates the shoulder on the protein peak which may be due to the Mo–MPT cofactor of NaR.

Table 2
Kinetic properties of purified S-NaR1 determined with two different electron donors: dithionite-reduced mv and dithionite-reduced BPB

Electron acceptor	Electron donor	Nitrate K_M (μM)	k_{cat} (s^{-1})	k_{cat}/K_M ($\text{s}^{-1} \mu\text{M}^{-1}$)
NO_3^-	MV	30 ± 3	159	5.3
NO_3^-	BPB	ND ^a	2081	69

^a Not determined, but assumed to be the same as determined with MV as electron donor.

tivity supported by MV is almost the same as when no electron-carrying dye is present and dithionite is directly reducing the Mo of the enzyme (data not shown). Thus, it is clear that BPB greatly enhances electron transfer to the Mo center in the nitrate reducing active site of

S-NaR1. This observation might not be true in holo-NaR, since the presence of the Cyt *b* domain could affect the redox potential of the Mo–MPT cofactor.

The determination of the apparent K_M for nitrate was performed with dithionite-reduced MV as electron donor and gave a value of $30 \pm 3 \mu\text{M}$ (see Table 2), which is close to the $40 \mu\text{M}$ value found for the holo-YNaR1 with NADH as electron donor (data not shown). Thus, the S-NaR1 fragment of YNaR1 retained the low K_M for nitrate, which is generally characteristic of eukaryotic NaR forms but not all [1]. This confirms that S-NaR1 is a highly efficient and specific nitrate-reducing catalyst and is illustrated by the k_{cat}/K_M value of $69 \text{ s}^{-1} \mu\text{M}^{-1}$ (Table 2), which is similar to the catalytic efficiency for nitrate reduction catalyzed by AtNR2 and other holo-NaR forms [1,10]. This demonstrates that S-NaR1 is fully capable of highly efficient nitrate reduction when electron supply is not limiting, despite the absence of the internal electron transfer system of the holo-NaR.

Cyclic voltammetry

To show that S-NaR1 could be reduced by electrons supplied at the surface of an electrode in the absence of an electron carrying dye, cyclic voltammetry was carried out. Sets of cyclic voltammograms of pyrolytic graphite electrodes prepared with a protein film containing either commercial natural corn leaf (*Z. mays*) NADH:NaR (ZmNaR1) or S-NaR1 in the presence and absence of nitrate ions in an anaerobic buffered system were performed at various potentials compared to the standard hydrogen electrode (Fig. 9). The direct electrical current traces shown in Fig. 9 demonstrate an enhanced response for the enzymes in the presence of nitrate ions, which indicated the nitrate

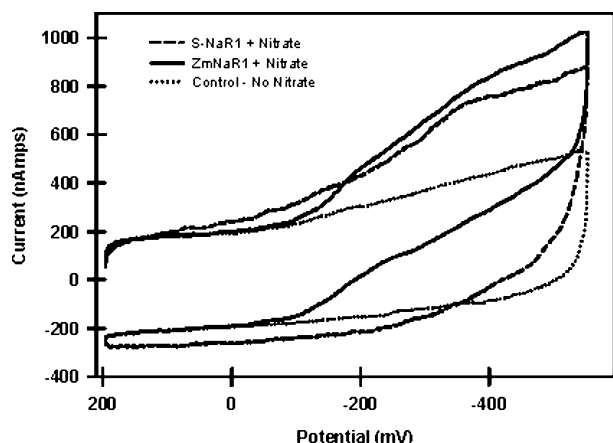


Fig. 9. Cyclic voltammograms comparing the nitrate-driven catalytic response of S-NaR1 and ZmNaR1 to a control for each enzyme which was analyzed in the absence of nitrate and normalized. The enzymes were present as a thin protein film on a edge-plane pyrolytic graphite electrode.

reducing catalytic activity of the enzymes. When nitrate ions were replaced by chloride or nitrite, no current was found. Azide, a known NaR inhibitor [1], blocked the current found in the presence of nitrate. Therefore S-NaR1, as well as the holo-enzyme, can use electrons provided by direct electric current for nitrate reduction in a specific way, and the product of the reaction, nitrite, does not seem to interfere with the reaction.

Conclusion

In conclusion, a simplified form of a eukaryotic NaR (S-NaR1) from the yeast *P. angusta* was engineered and expressed at high level by fermentation in the phylogenically similar yeast *P. pastoris*. The active S-NaR1 contained only the polypeptide for the nitrate-reducing fragment which contained the Mo–MPT cofactor binding site. The host *P. pastoris* supplied the Mo–MPT cofactor to the S-NaR1 polypeptide to form the active nitrate-reducing catalyst. Purified S-NaR1 was most capable of nitrate reduction when electrons were donated via dithionite-reduced BPB under the conditions used here. The S-NaR1 monomer had an M_R of 55 kDa determined by SDS–PAGE, which is very close to the predicted size for the polypeptide. The most common active form of the active catalytic protein appeared to be homo-tetrameric according to the gel exclusion chromatography. The active purified S-NaR1 had a nitrate K_M of $30 \pm 3 \mu\text{M}$ and an enzyme efficiency comparable to those of the natural and recombinant forms of holo-NaR. This active fragment of NaR confirms the hypothesis that the domains and major fragments of the holo-NaR are functionally and structurally independent.

Nitrate pollution is a problem worldwide and the lack of a sensitive affordable field nitrate sensor has made continuous monitoring of nitrate levels in natural waters virtually impossible [1]. However, since the cyclic voltammetry experiments showed that the nitrate reduction of simplified nitrate reductase is highly specific and can be driven by an electrical current without a dye mediator, this enzyme fragment could be ideal for development of a nitrate biosensor.

Acknowledgments

We thank Troy Kinnunen-Skidmore and Benedicte Chommeloux for assistance with the experiments. We also thank Prof. James M. Cregg for supplying the wild-type *P. pastoris* strain Y-11430 and Prof. Jose M. Siverio for the kind gift of the YNaR1 containing plasmid. This work was supported in part by an NIH SBIR grant to NECi (Contract #R44GM56598).

References

- [1] W.H. Campbell, Nitrate reductase, function and regulation: bridging the gap between biochemistry and physiology, *Annu. Rev. Plant Physiol. Plant Mol. Biol.* 50 (1999) 277–303.
- [2] M.G. Redinbaugh, W.H. Campbell, Quaternary structure and composition of squash NADH:nitrate reductase, *J. Biol. Chem.* 260 (1985) 3380–3385.
- [3] R. Hille, Mechanistic aspects of the mononuclear molybdenum enzymes, *J. Biol. Inorg. Chem.* 2 (1997) 804–809.
- [4] C. Kisker, H. Shindelin, D.C. Rees, Molybdenum-containing enzymes: structure and mechanism, *Annu. Rev. Biochem.* 66 (1997) 233–267.
- [5] C. Kisker, H. Shindelin, A. Pacheco, W.A. Webhi, R.M. Garret, K.V. Rajagopalan, J.H. Enemark, D.C. Rees, Molecular basis of sulfite oxidase deficiency from the structure of sulfite oxidase, *Cell* 91 (1997) 973–983.
- [6] W. Su, J.A. Mertens, K. Kanamaru, W.H. Campbell, N.M. Crawford, Analysis of wild-type and mutant plant nitrate reductase expressed in the methylotrophic yeast *Pichia pastoris*, *Plant Physiol.* 115 (1997) 1135–1143.
- [7] J. Avila, M.D. Perez, N. Brito, C. Gonzales, J.M. Siverio, Cloning and disruption of the YNR1 gene encoding the nitrate reductase apoenzyme of the yeast *Hansenula polymorpha*, *FEBS Lett.* 366 (1995) 137–142.
- [8] G.G. Barbier, W.H. Campbell, Expression of *Pichia angusta* nitrate reductase (YNaR1) in *Pichia pastoris*, in: *Current Topics in Gene Expression Systems: Program and Abstracts*, Abstract PY, vol. 4, 2000, p. 64.
- [9] K. Kanamaru, R. Wang, W. Su, N.N. Crawford, Ser-534 in the hinge 1 region of *Arabidopsis* nitrate reductase is conditionally required for binding of 14-3-3 proteins in vitro inhibition, *J. Biol. Chem.* 274 (1999) 4160–4165.
- [10] L. Skipper, J.A. Mertens, W.H. Campbell, D.J. Lowe, Pre-steady-state kinetics analysis of recombinant *Arabidopsis* NADH:nitrate reductase, *J. Biol. Chem.* 276 (2001) 26995–27002.
- [11] A. Pacheco, J.T. Hazzard, G. Tollin, J.H. Enemark, The pH dependence of intramolecular electron transfer rates in sulfite oxidase at high and low anion concentrations, *J. Biol. Inorg. Chem.* 4 (1999) 390–401.
- [12] G.N. George, J.A. Mertens, W.H. Campbell, Structural changes induced by catalytic turnover at the molybdenum site of *Arabidopsis* nitrate reductase, *J. Am. Chem. Soc.* 121 (1999) 9730–9731.
- [13] G.E. Hyde, W.H. Campbell, High-level expression in *Escherichia coli* of the catalytically active flavin domain of corn leaf NADH:nitrate reductase and its comparison to human NADH:cytochrome *b*₅ reductase, *Biochem. Biophys. Res. Commun.* 168 (1990) 1285–1291.
- [14] G. Lu, Y. Lindqvist, G. Schneider, U. Dwivedi, W.H. Campbell, Structural studies on corn nitrate reductase: refined structure of the cytochrome *b* reductase fragment at 2.5 Å, its ADP complex and an active-site mutant and modeling of the cytochrome *b* domain, *J. Mol. Biol.* 248 (1995) 931–948.
- [15] W.H. Campbell, Expression in *Escherichia coli* of cytochrome *c* reductase activity from a maize NADH:Nitrate reductase cDNA, *Plant Physiol.* 99 (1992) 693–699.
- [16] J.A. Mertens, N. Shiraishi, W.H. Campbell, Recombinant expression of molybdenum reductase fragments of plant nitrate reductase at high levels in *Pichia pastoris*, *Plant Physiol.* 123 (2000) 743–756.
- [17] G.B. Quinn, A.J. Trimboli, M.J. Barber, Construction and expression of a flavocytochrome *b*₅ chimera, *J. Biol. Chem.* 269 (1994) 13375–13381.
- [18] S.A. Glazier, E.R. Campbell, W.H. Campbell, Construction and characterization of nitrate reductase-based amperometric electrode and nitrate assay of fertilizers and drinking water, *Anal. Chem.* 70 (1998) 1511–1515.
- [19] D.R. Higgins, J.M. Cregg, Introduction to *Pichia pastoris*, in: D.R. Higgins, J.M. Cregg (Eds.), *Pichia* Protocols, Humana Press, NJ, 1998, pp. 1–15.
- [20] M. Romanos, C. Scorer, K. Sreekrishna, J. Clare, The generation of multicopy recombinant strains, in: D.R. Higgins, J.M. Cregg (Eds.), *Pichia* Protocols, Humana Press, NJ, 1998, pp. 55–72.
- [21] J. Clare, K. Sreekrishna, M. Romanos, Expression of tetanus toxin fragment C, in: D.R. Higgins, J.M. Cregg (Eds.), *Pichia* Protocols, Humana Press, NJ, 1998, pp. 193–208.
- [22] J. Stratton, V. Chiruvulu, M. Meagher, High cell-density fermentation, in: D.R. Higgins, J.M. Cregg (Eds.), *Pichia* Protocols, Humana Press, NJ/NY, 1998, pp. 107–120.
- [23] K.L. Turner, M.K. Doherty, H.A. Heering, F.A. Armstrong, G.A. Reid, S.K. Chapman, Redox properties of flavocytochrome *c*₃ from *Shewanella frigidimarina* NCIMB400, *Biochemistry* 38 (1999) 3302–3313.
- [24] A. Vassileva, D.A. Chugh, S. Swaminathan, N. Khanna, Effect of copy number on the expression levels of hepatitis B surface antigen in the methylotrophic yeast *Pichia pastoris*, *Protein Expr. Purif.* 21 (2001) 71–80.